Turkdogan, E. T., R. G. Olsson, and J. V. Vinters, "Gaseous Reduction of Iron Oxides, Part II: Pore Characteristics of Iron Reduced from Hematite in Hydrogen," *ibid.*, **2**, 3189 (1971).
Turkdogan, E. T. and J. V. Vinters, "Reducibility of Iron Ore Pellets and Effect of Additions," *Can. Met. Quart.*, **12**, 9 (1973).
Warner, N. A., "Reduction Kinetics of Hematite and the Influence of Gaseous Diffusion," *TMS-AIME*, **230**, 163 (1964*a*).
Warner, N. A., "Kinetics of the Gaseous Reduction of Hematite," *Proc. Australas. Inst. Min. Metall.*, No. 210, 31 (1964*b*).

Manuscript received July 12, and accepted September 1, 1976.

Part II. The Direct Reduction Process in a Shaft Furnace Arrangement

A mathematical model was developed for the direct reduction of hematite carried out in a countercurrent moving packed bed, and the process was simulated on a CDC 6400 computer. The response of the model to changes in the various process variables was investigated, and it was found that there is an optimum gas inlet composition (hydrogen-carbon monoxide) for a given set of operating conditions. In addition, an optimum gas inlet temperature was revealed for cases where pure carbon monoxide was used as the reducing gas. The feasibility of side stream injection of reducing gas was studied. The calculations showed that there are certain ranges of operating conditions for which the injection of a hot side stream is advantageous. This study represents the first reported simulation of direct reduction process having carbon monoxide-hydrogen gas mixtures as a reducing medium.

SCOPE

This work represents the first published study of the direct reduction of ferric oxide pellets in a nonisothermal shaft reactor using carbon monoxide plus hydrogen gas mixtures. The kinetic model for the reduction process, developed and verified experimentally in Part I, forms the basis of the reactor model and lends credibility to the simulation results. The system response to operating changes and the discovery of optimal inlet gas compositions, temperatures, etc., should be of interest to the industrial practitioner.

CONCLUSIONS AND SIGNIFICANCE

A mathematical model for the direct reduction process carried out in a countercurrent moving bed using carbon monoxide plus hydrogen mixtures was developed and the response of the model to changes in the various process variables determined. The results show that there exists an optimum inlet gas composition (carbon monoxide-hydrogen) which shifts in response to changes in the other operating conditions. For carbon monoxide-hematite systems, especially those cases using small gas feed rates, there also exists an optimum gas inlet temperature. The feasibility of side stream injection of reducing gas was studied. It was found that there are only certain ranges of operating conditions for which the injection of a side stream would be desirable.

The results of this work suggest several areas in which further optimization studies should be made in order to improve the operation of commercial direct reduction processes.

The projected demands for steel in the coming years coupled with the changing economics in the steel industry strongly support the need for prereduced iron as feedstock (Mackenzie, 1963; Lownie and Barnes, 1972; J. R. Miller, 1972; Pitt, 1973*a-b*). The development of widely accepted prereduction technology is therefore important. More than fifty techniques have been developed for the direct reduction of iron ore, but few have developed beyond the pilot plant stage (McGannon, 1971). In the literature a large number of kinetic studies on a single particle placed in a given environment have been reported over the last 20 yr (see Part I for a discussion of these). However, few attempts have been made to analyze the behavior of metallurgical shaft reactors where the gaseous reduction of hematite takes place. Previous studies on these packed-bed reactors include the work of Barner (1963) and Yagi et al. (1971), who studied isothermal reactors, and the work of Yagi (1974) on nonisothermal reactors. These authors made use of an unreacted shrinking core model (single interface model) to simulate the reduction process. Spitzer et al. (1968) simulated the process in a countercurrent moving packed bed under isothermal conditions by em-

ploying a three-interface model, where hydrogen was the reducing gas. R. L. Miller (1972) developed a model for hematite reduction by carbon dioxide in an adiabatic moving packed bed. He used a simplified three-interface model for pellets which excluded the gaseous diffusion resistances through the gas film and the product layers while lumping them into the interfacial resistances. Consequently, the rate of reduction calculated by him was faster than normally observed values. In contrast to these studies, the reducing gas used in industry for the direct reduction process is neither pure hydrogen nor pure carbon monoxide gas; instead, it is a mixture, consisting of mainly hydrogen and carbon monoxide, which is obtained from partially oxidized natural gas or natural gas reformed by steam (Cruse et al., 1969; McGannon, 1971; Labee, 1974). Thus there is a definite need for a simulation study of the shaft furnace for the case of carbon monoxide-hydrogen gas mixtures.

In the present paper, a detailed mathematical model is developed for direct reduction process carried out in a countercurrent moving packed bed using hydrogen plus carbon monoxide mixtures. The model incorporates the three-interface single pellet model which was formulated and validated with experimental data in Part I. Through the use of this model, the influence of process operating conditions on the shaft furnace will be determined, several potential operating innovations will be tested, and suggestions for improved furnace design will be formulated. It is expected that these results will be of value in the future design of direct reduction reactors as well as in carrying out the optimization of existing commercial processes.

THE PROCESS DESCRIPTION

In the present work we consider the direct reduction unit to consist of a moving packed bed as sketched in Figure 1. Pellets are loaded at the top of the bed and move countercurrent to a reducing gas which is injected at the bottom (and which may also be injected sidestream). The reduced iron is removed as product at the bottom, and the spent gas coming from the top may be regenerated and recycled.

In the present mathematical model for the process, we make the following assumptions:

1. Steady state, adiabatic operation of the reactor.
2. Both the gas and solid move in plug flow with negligible axial and radial dispersion.
3. The bed is uniform radially.
4. The pellets are spherical with constant, uniform size and react according to the kinetics established in Part I.
5. Ideal gas behavior with no gas phase side reactions.
6. Instantaneous mixing occurs radially at a sidestream injection point.

With these assumptions, the mathematical model includes a gas material balance

$$-G\frac{dy_{CO}^{b}}{dz} = \phi^{(h\text{-}m)}R_{CO}^{(h\text{-}m)} + \phi^{(m\text{-}w)}R_{CO}^{(m\text{-}w)} + \phi^{(w\text{-}Fe)}R_{CO}^{(w\text{-}Fe)} \quad (1)$$

$$-G\frac{dy_{H_2}^{b}}{dz} = \phi^{(h\text{-}m)}R_{H_2}^{(h\text{-}m)} + \phi^{(m\text{-}w)}R_{H_2}^{(m\text{-}w)} + \phi^{(w\text{-}Fe)}R_{H_2}^{(w\text{-}Fe)} \quad (2)$$

which requires that the reducing gas (carbon monoxide or hydrogen) consumed in the bulk gas phase be equal to the sum of the relevant gas-solid reaction rates at three

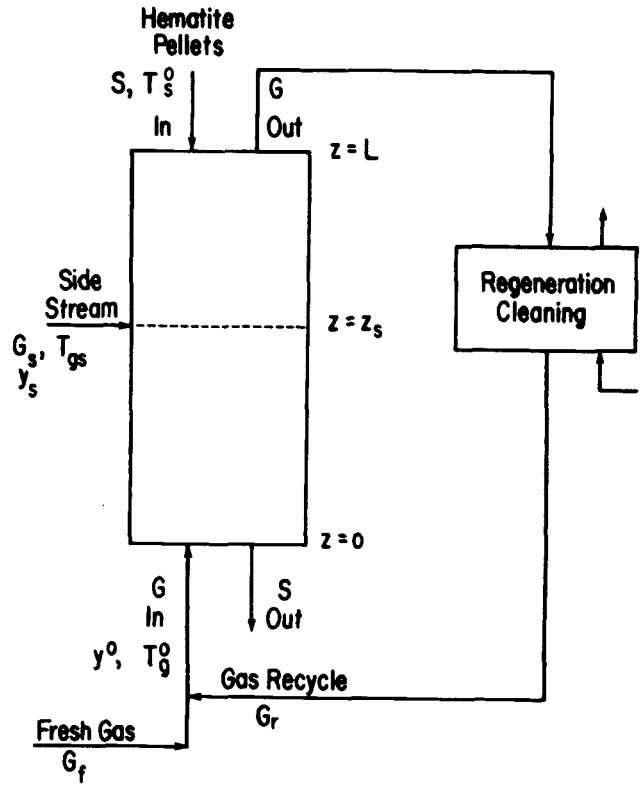

Fig. 1. Schematic representation of the direct reduction process with gas recycle.

individual interfaces, hematite/magnetite/wustite/iron, within the pellets. The interface positions of pellets at any point in the bed z are given by

$$\frac{dx^{(t\text{-}s)}}{dz} = \frac{P}{\rho_t \phi^{(t\text{-}s)}(1-\epsilon_t)RT_s u_s}\left[k_{r,CO}^{(t\text{-}s)}\left(y_{CO}^{(t\text{-}s)} - \frac{1-y_{CO}^{(t\text{-}s)}}{K_{e,CO}^{(t\text{-}s)}} \right) + k_{r,H_2}^{(t\text{-}s)}\left(y_{H_2}^{(t\text{-}s)} - \frac{1-y_{H_2}^{(t\text{-}s)}}{K_{e,H_2}^{(t\text{-}s)}} \right) \right] \quad (3)$$

where the particular interface t-s can be hematite/magnetite (h-m), magnetite/wustite (m-w), or wustite/iron (w-Fe). The internal gas phase compositions are given by

$$y_i^{(t\text{-}s)} = p_i^{(t\text{-}s)}/P \quad i: \text{CO or } H_2 \quad (4)$$

where $p_i^{(t\text{-}s)}$ is the partial pressure of the reactant i at the t-s interface calculated as shown in Part I. The receding rate of each interface toward the center of the pellets is the sum of the contributions from both carbon monoxide and hydrogen reacting with the oxide at the interface. Thus, Equation (3) represents three modeling equations for the receding rates of the interfaces for hematite/magnetite, magnetite/wustite, and wustite/iron, respectively.

In addition, one needs a gas phase heat balance

$$G\overline{C}_{pg}\frac{dT_g}{dz} = h\,a\,(T_s - T_g) \quad (5)$$

which shows that the temperature change of the bulk gas phase in the axial direction is due only to the effect of heat transfer from the pellets. Furthermore, the heat balance on the solids is written as

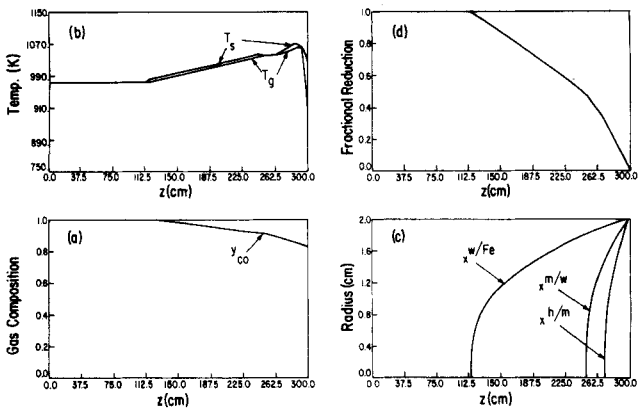

Fig. 2. Typical computed temperature and composition profiles for reduction with hydrogen.

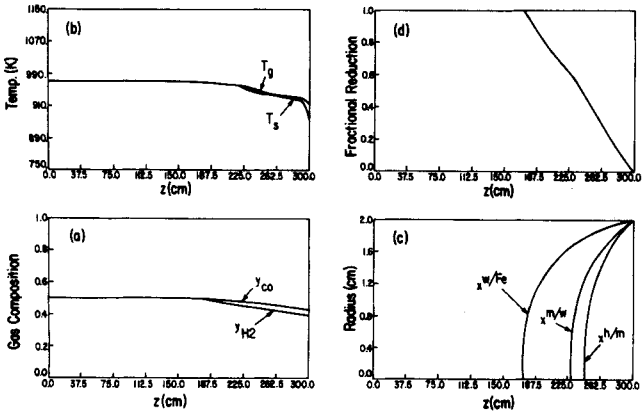

Fig. 4. Typical temperature and composition profiles for reduction with a gas mixture consisting initially of 50% hydrogen and 50% carbon monoxide.

$$(1-\epsilon_b)\,u_s\,\overline{\rho_s C_{ps}}\,\frac{dT_s}{dz} = h\,a\,(T_g - T_s) + \Delta H_{CO}^{(h\text{-}m)} R_{CO}^{(h\text{-}m)} + \Delta H_{CO}^{(m\text{-}w)} R_{CO}^{(m\text{-}w)} + \Delta H_{CO}^{(w\text{-}Fe)} R_{CO}^{(w\text{-}Fe)} + \Delta H_{H_2}^{(h\text{-}m)} R_{H_2}^{(h\text{-}m)} + \Delta H_{H_2}^{(m\text{-}w)} R_{H_2}^{(m\text{-}w)} + \Delta H_{H_2}^{(w\text{-}Fe)} R_{H_2}^{(w\text{-}Fe)} \quad (6)$$

where

$$\overline{\rho_s C_{ps}} = \rho_h C_{ph}(1-\epsilon_h)\left[\frac{x^{(h\text{-}m)}}{x_o}\right]^3 + \rho_m C_{pm}(1-\epsilon_m)\left[\frac{[x^{(m\text{-}w)}]^3 - [x^{(h\text{-}m)}]^3}{x_o^3}\right] + \rho_w C_{pw}(1-\epsilon_w)\left[\frac{[x^{(w\text{-}Fe)}]^3 - [x^{(m\text{-}w)}]^3}{x_o^3}\right] + \rho_{Fe} C_{pFe}(1-\epsilon_{Fe})\left[1-\left[\frac{x^{(w\text{-}Fe)}}{x_o}\right]^3\right] \quad (7)$$

and

$$R^{(t\text{-}s)} = \frac{3(1-\epsilon_b)}{x_o^3}\cdot\frac{[x^{(t\text{-}s)}]^2\,P\phi^{(t\text{-}s)}k_r^{(t\text{-}s)}}{RT_s}\cdot\left[y^{(t\text{-}s)} - \frac{1-y^{(t\text{-}s)}}{K_e^{(t\text{-}s)}}\right] \quad (8)$$

represents the reaction rate at the (h-m), (m-w), or (w-Fe) interface. The temperature change of the pellets along the axial direction of the bed is due to the sum of the heat transfer from the surrounding gas phase into the pellets and the thermodynamic heat effects resulting from carbon monoxide and hydrogen reacting with the iron oxides. Within each pellet, the temperature is assumed homogeneously distributed because of the high values of heat conductivities of iron and its oxides (Perry, 1963; Weast, 1973) which make the temperature drop within the pellet negligible in comparison with that across the gas film around the pellet.

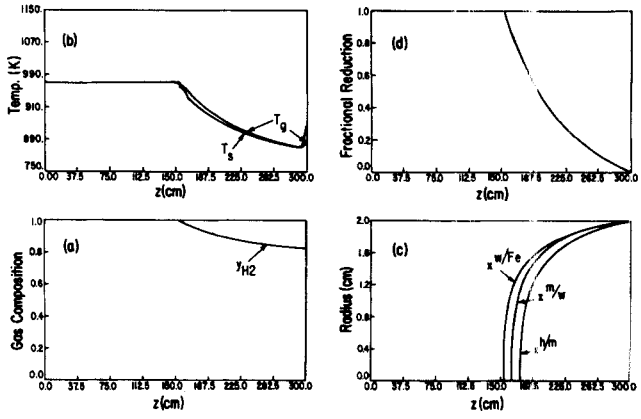

Fig. 3. Typical temperature and composition profiles for reduction with carbon monoxide.

The boundary conditions for the model are as follows:

At bottom of the bed

$$y_{CO}^{b}(0) = y_{CO}^{bo} \quad (9)$$

$$y_{H_2}^{b}(0) = y_{H_2}^{bo} \quad (10)$$

$$T_g(0) = T_g^{o} \quad (11)$$

At top of the bed

$$x^{(h\text{-}m)}(L) = x_o \quad (12)$$

$$x^{(m\text{-}w)}(L) = x_o \quad (13)$$

$$x^{(w\text{-}Fe)}(L) = x_o \quad (14)$$

$$T_s(L) = T_s^{o} \quad (15)$$

In some instances, it may be advantageous to inject a sidestream of reducing gas. For an injection at point $z = z_s$, there are auxiliary conditions on the total gas flow, gas composition, and gas enthalpy which must be satisfied:

$$G(z_{s+}) = G(z_{s-}) + G_s \quad (16)$$

$$G\,y_i|_{z=z_{s+}} = G\,y_i|_{z=z_{s-}} + G_s\,y_{is} \quad (17)$$

$$G\,\overline{H}|_{z=z_{s+}} = G\,\overline{H}|_{z=z_{s-}} + G_s\,H_s \quad (18)$$

where G_s, y_{is}, H_s represent the sidestream injection rate, sidestream composition, and sidestream enthalpy, respectively.

THE MODEL PREDICTIONS

The mathematical model calculations required the solution of seven ordinary differential equations having split boundary conditions (three at the bottom and four at the top of the reactor). This two-point boundary value problem was solved by guessing the missing boundary conditions at the top of the bed and integrating downward to produce values at the bottom of the bed. A least-squares optimization procedure (Tsay, 1975) was used to iterate and cause the boundary conditions to be satisfied. One complete simulation required approximately 3 to 4 min on the CDC 6400 computer.

TABLE 1. NOMINAL OPERATING CONDITIONS

1. Simulation conditions of the bed
   Void fraction of the pellets (ϵ_h): 0.2
   Void fraction of the bed (ϵ_b): 0.38
   Length of the bed (L): 300 cm
   Diameter of the bed (D): 15 cm
   Solid pellets downflow velocity (u_s): -0.0105 cm/s (-0.0026 hematite-tons/day-cm^2)
   Gas upflow rate (G): 4.15 l/min-cm^2 at 25°C and 1 atm
   Flow rate ratio of hematite to gas: 0.06 (mole basis)
   Atmosphere: 1 atm
2. Boundary conditions

Top (L)	Solid temperature (T_s^o): 873°K	
	Pellet radius (x_o): 2 cm	
Bottom (0)	Gas temperature (T_g^o): 973°K	
	Gas composition (y^{bo}): CO, 50%CO-50%H_2, H_2	

TABLE 2. RANGES OF PROCESS VARIABLES STUDIED

1. Simulation conditions of the bed
   Void fraction of the bed: 0.38
   Void fraction of the pellet: 0.0 ~ 0.3
   Length of the bed: 80 ~ 700 cm
   Diameter of the bed: 15 ~ 30 cm
   Solid pellet downflow rate: 0.01 ~ 0.1 cm/s ($1.5 \sim 15.0 \times 10^{-4}$ g-mole Fe_2O_3/s-cm^2)
   Gas upflow rate: 2.49 ~ 24.9 l/min-cm^2 at 25°C (1.7 ~ 17.0 g-mole/s-cm^2)
   Atmosphere pressure: 1 atm
2. Boundary conditions

Top	Solid feed temperature: 850° ~ 1 100°K
	Pellet radius: 0.5 ~ 5.0 cm
Bottom	Gas feed temperature: 850° ~ 1 600°K
	Gas feed composition: various compositions of H_2-CO mixtures

3. Side stream
   Temperature: 850° ~ 2 100°K
   Gas composition: various compositions of H_2-CO mixtures
   Ratio of side stream to total gas flow rate: 0.0 ~ 0.4
   Location: various levels along the bed

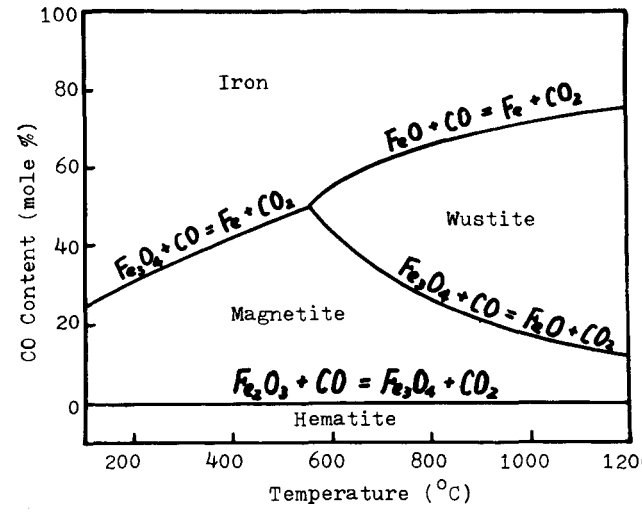

Equilibrium of Iron-Oxygen-Carbon System at 1 atm.

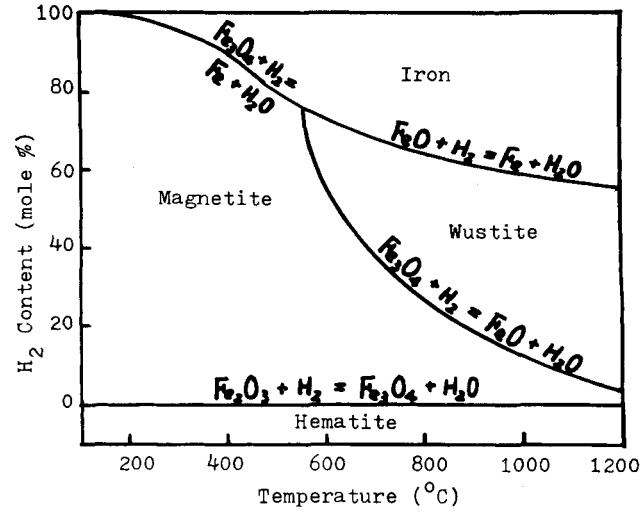

Equilibrium of Iron-Oxygen-Hydrogen System at 1 atm.

Fig. 5. Equilibrium diagrams.
(a) Iron-oxygen-hydrogen system.
(b) Iron-oxygen-carbon monoxide.

A set of nominal operating conditions (shown in Table 1) were chosen to study the typical behavior of the reduction unit. The model predictions under these conditions are shown in Figures 2 to 4 for pure carbon monoxide, pure hydrogen, and for a 50-50 gas mixture in the feed. For carbon monoxide as a reducing gas, the process is exothermic, and the slowest step is seen to be the movement of the wustite/iron interface. This is due to the unfortunate combination of a temperature rise in the bed (Figure 2*a*) which induces a strong equilibrium limitation in the rate of wustite reduction (Figure 5*a*). For pure hydrogen, on the other hand, the rates of reduction are much faster than for carbon monoxide for single pellets (see Part I). However, the process is endothermic, and the resulting temperature drop in the bed (Figure 3*a*) is detrimental from both the kinetic and equilibrium points of view. In addition, the process is close to the equilibrium triple point in Figure 5*b*, so that all three interfaces move almost together. For the conditions considered, a gas mixture of about 50% hydrogen-50% carbon monoxide appears to be better than for either pure gas. By combining exothermic and endothermic reactions, the bed temperature is in the desired range so that a better combination of kinetic and equilibrium conditions arises. It follows that there should exist an optimal feed composition for the system.

In order to determine the effects of changing operating conditions, a number of perturbations were made around the nominal operating conditions shown in Table 1. The range of variables studied are listed in Table 2. Although the detailed results are available (Tsay, 1975), only a summary of these will be presented here.

As would be expected, an increase in the reactor residence time (through a lengthened reactor or reduced solids flow rate) increases the extent of conversion, provided the reducing gas concentration is kept above the equilibrium value. If the reducing gas reaches its equilibrium value (Figure 5), no amount of residence time increase will improve conversion.

Similarly, a reduction of the pellet diameter increases the reduction rate due to the increased surface to volume ratio. However, practical considerations such as pressure drop, onset of fluidization, etc., would establish a lower bound on the desirable pellet size.

An increase of the gas feed rate increases the gas concentration as well as the pellet-gas heat and mass transfer coefficients. Thus, the overall effect of such an increase is to increase the reaction rate, chiefly through providing a higher reducing potential in the bed.

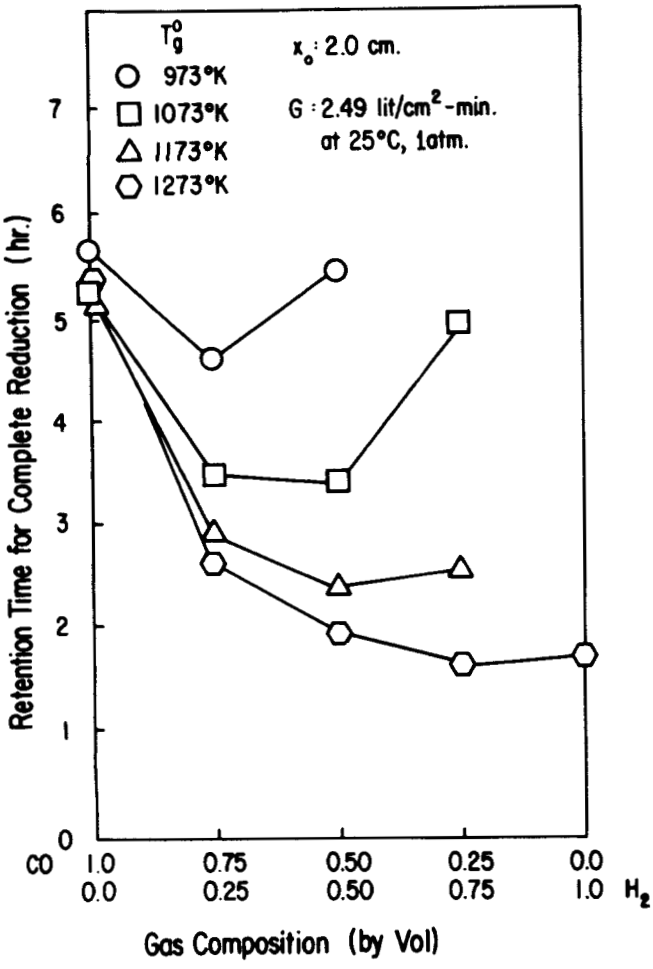

Fig. 6. Calculation of the optimal gas feed composition.

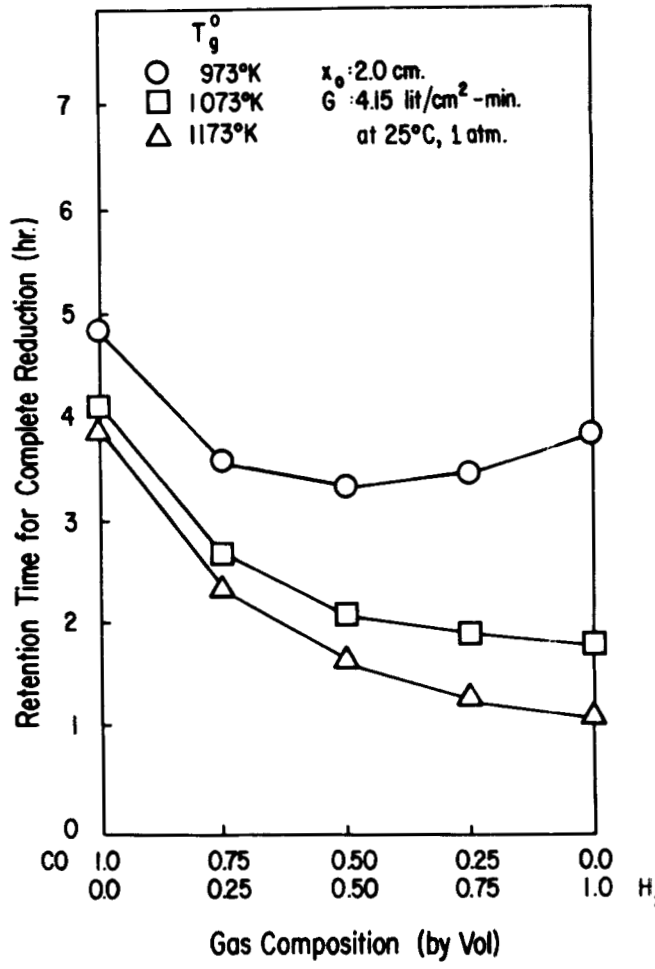

Fig. 7. Calculation of the optimal gas feed composition.

The remaining variables, the gas feed temperature, the gas feed concentration, and the solid feed temperature were found to have strong interactions in their effects. Since preheating of the solid in a nonoxidizing atmosphere is less likely to be practical than heating the gas stream, we shall concentrate our attention on the effects of adjusting gas feed temperature and composition.

The overall goal in choosing the best combination of gas feed composition and gas feed temperature is to avoid very high temperatures which lead to sintering or even melting of the solid as well as causing conversion losses with a carbon monoxide rich gas stream. For these reasons, most existing direct reduction processes operate below 1 100°C (Cruse et al., 1969; McGannon, 1971; Labee, 1974). At the same time, very low temperatures and low reducing potential for the gas are to be avoided because these limit the rate kinetically as well as causing equilibrium limitations.

To investigate the best combination of gas feed temperature and gas feed composition, a number of simulations were carried out. The results of these simulations, shown in Figures 6 to 9, are quite interesting. Figures 6 and 7 are for a relatively large pellet size and at different gas feed rates. In each of the figures, the optimum gas composition shifts towards more hydrogen at higher feed temperatures and moves towards carbon monoxide at lower feed temperatures. In this way, the heat generated by carbon monoxide and heat consumed by hydrogen are balanced to provide a good temperature level at any gas inlet temperature. Higher gas feed rates and larger pellets tend to shift the optimal gas composition towards higher hydrogen content. This is because higher gas feed rates can provide more heat and a higher reducing potential so as to take advantage of the higher rates of reaction using pure hydrogen while overcoming some of the disadvantages of the endothermic reaction. When faced with larger pellets, the much higher diffusivity of hydrogen is chosen so as to overcome the larger gas transport resistance inherent in operation with larger pellets.

The simulations also showed that an optimum exists for the gas feed temperature when pure carbon monoxide is fed (Figure 10). This observation is readily explained if one recalls that carbon monoxide reduction is exothermic and must be governed by the equilibrium diagram given in Figure 5. At very low temperatures, the kinetic rate is low, while at very high temperatures, the reaction rate is equilibrium limited. Although the calculations were not performed, this effect should also arise for feed gas mixtures having a relatively large carbon monoxide content.

As has been mentioned above, there may be instances where the use of a side stream injection to adjust the temperature and composition at some point in the bed would be advantageous. To investigate this possibility, a limited number of simulations were carried out with the model. Figures 11 and 12 show the extent of reduction in a 200 cm bed as a function of the side stream location for the cases of pure hydrogen and pure carbon monoxide, respectively. In the case of pure hydrogen, the side stream chosen had a high temperature, and there was a small advantage in using it close to the bottom of the bed. However, for carbon monoxide there seemed to be no advantage for the case studied. Clearly, for any specific process, the feasible range of side stream compositions, temperatures, and in-

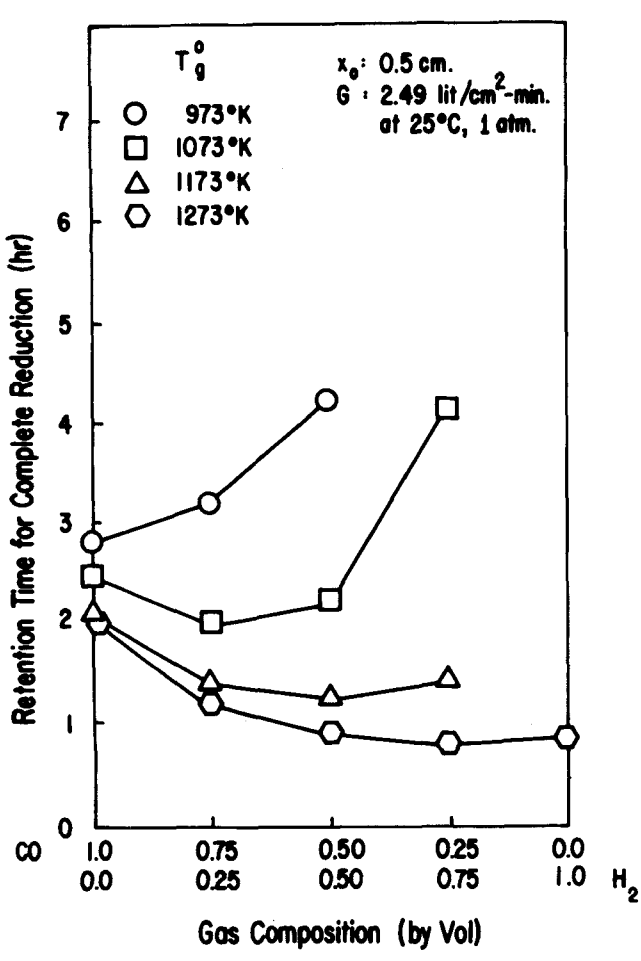

Fig. 8. Calculation of the optimal gas feed composition.

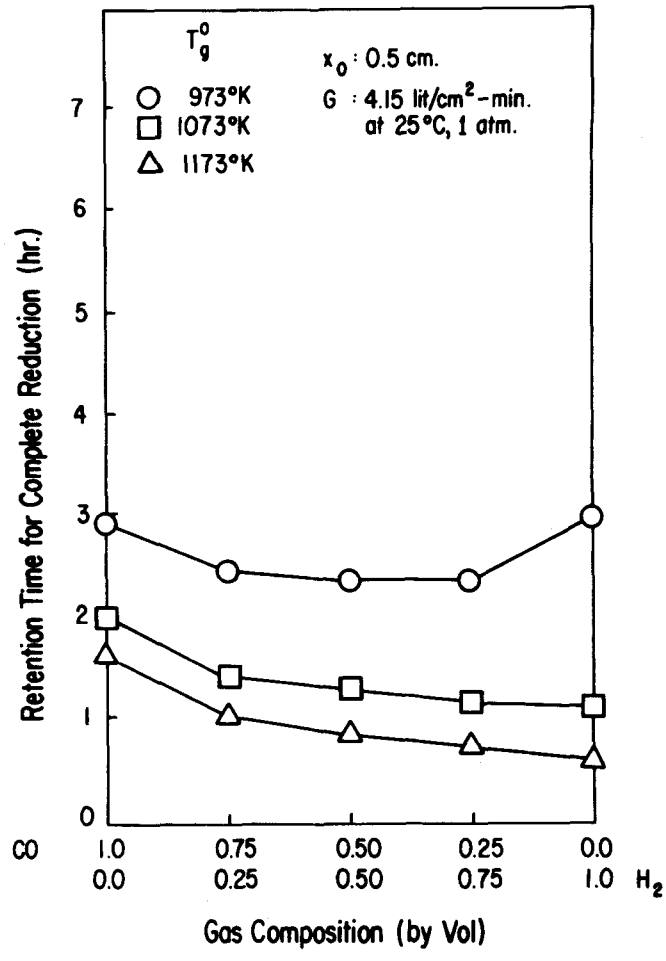

Fig. 9. Calculation of the optimal gas feed composition.

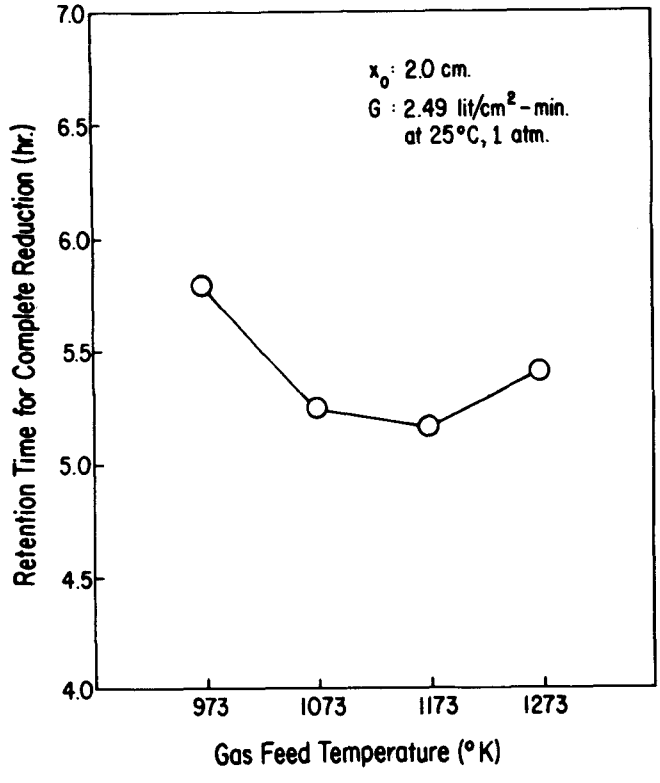

Fig. 10. Calculation of the optimal gas inlet temperature.

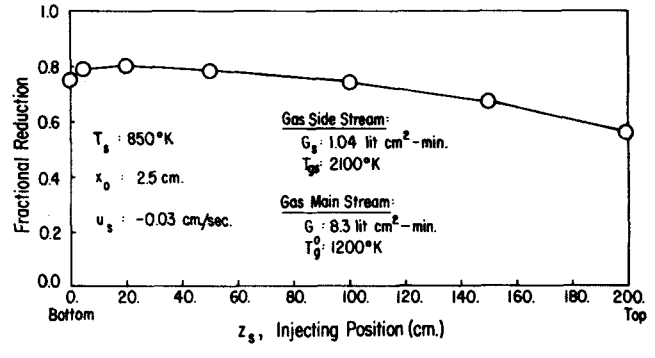

Fig. 11. Plot of the final yield as a function of the position of side stream injection for reducton with hydrogen.

jection rates could be studied through simulation by making use of a model such as developed here.

CONCLUDING REMARKS

A number of interesting points have arisen from our modeling study of the direct reduction process. It has been demonstrated that the model is compatible with the single pellet kinetic studies reported in Part I, and thus the trends found should represent the expected behavior of actual direct reduction units. For these reasons, the present results should be relevant to both the design of new direct reduction units and to the optimization of existing installations.

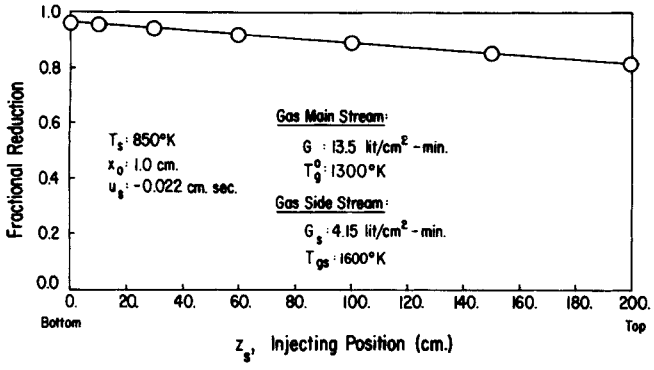

Fig. 12. Plot of the final yield as a function of the position of side stream injection for reduction with carbon monoxide.

The computed results indicate that there is an optimal gaseous feed composition which depends on the gas flow rate, feed temperature, and on the diameter of the hematite pellets. In commercial operation, such as in the Armco Process (Cruse et al., 1969; Labee, 1974), the reducing gases are produced by the partial oxidation of natural gas. In this reformer, the product gases are approximately in the ratio 3 hydrogen/carbon monoxide with water, carbon dioxide, and methane being minor constituents. It is extremely interesting that this corresponds quite closely to the optimum gas composition for a feed temperature of 1 273°K in Figures 6 and 8 and is near optimal in the other figures for gas feed temperatures in the commercial range. Thus it would appear that fortuitously many direct reduction units may be operating close to the optimum feed composition, although further improvements through optimization studies are quite likely.

ACKNOWLEDGMENT

The authors wish to thank the National Science Foundation, RANN Division, for partial support of this investigation.

NOTATION

a = total particle surface area per unit bed volume, cm²/cm³
C_{pg} = specific heat of gas, cal/gmole-°K
C_{pt} = specific heat of solid phase t, cal/gmole-°K
D = diameter of the bed, cm
G = gas flow rate of main stream, gmole/cm²-s
G_s = gas flow rate of side stream, gmole/s
$G(z_s-)$ = upstream gas flow rate before side stream is injected at z_s, gmole/cm²-s
$G(z_s+)$ = downstream gas flow rate after side stream is injected at z_s, gmole/cm²-s
h = heat transfer coefficient around surface of pellets, cal/cm²-s-°K
H = enthalpy, cal/gmole
$\Delta H^{(t\text{-}s)}$ = enthalpy change from t to s species per unit volume of bed, cal/cm³
H_s = enthalpy of side stream, cal/gmole
$\overline{H}(z_s-)$ = upstream enthalpy before side stream is injected at z_s, cal/gmole
$\overline{H}(z_s+)$ = downstream enthalpy after side stream is injected at z_s, cal/gmole
$k_r^{(t\text{-}s)}$ = specific rate constant for reaction from t to s species, cm/s
$K_e^{(t\text{-}s)}$ = equilibrium constant for reaction from t to s species, dimensionless
L = length of bed, cm
$p_i^{(t\text{-}s)}$ = partial pressure of gas component at the interface, t-s, atm
P = atmosphere pressure, atm
R = gas constant
$R^{(t\text{-}s)}$ = reaction rate from t to s per unit volume of bed, gmole/s-cm³
T = temperature, °K
T_g = gas temperature, °K
T_g^o = gas feed temperature, °K
T_{gs} = gas side stream temperature, °K
T_s = solid temperature, °K
T_s^o = solid feed temperature, °K
u_s = solid downflow velocity, cm/s
x_o = pellet size in radius, cm
$x^{(t\text{-}s)}$ = effective radius of interface between t and s species, cm
y_i = molar fraction of gas component i, dimensionless
y_{is} = molar fraction of gas component i in side stream, dimensionless
$y_i(z_s-)$ = molar fraction of gas component i in main stream before side stream is injected at z_s, dimensionless
$y_i(z_s+)$ = molar fraction of gas component i in main stream after side stream is injected at z_s, dimensionless
y_i^b = molar fraction of gas component i in bulk phase, dimensionless
y_i^{bo} = molar fraction of gas component i in bulk phase of inlet gas stream, dimensionless
$y_i^{(t\text{-}s)}$ = molar fraction of gas component i at the interface between t and s species, dimensionless
z = distance from the bottom of the bed, cm
z_s = injecting level of side stream, cm
ϵ_b = void fraction of the bed, dimensionless
ϵ_t = void fraction of t phase, dimensionless
ρ_t = true molar density of t species, gmole/cm³
$\phi^{(t\text{-}s)}$ = oxygen density change from t to s species, $\phi^{(h\text{-}m)} = 0.333$, $\phi^{(m\text{-}w)} = 0.832$, $\phi^{(h\text{-}w)} = 0.888$, $\phi^{(w\text{-}Fe)} = 1.00$, 0 atom/gmole t

Subscripts

h = hematite
m = magnetite
w = wustite
Fe = iron

LITERATURE CITED

Barner, H. E., "Theoretical Analysis of Hydrogen Reduction of Hematite in a Fixed Bed," *TMS-AIME*, 227, 897 (1963).

Cruse, C. L., A. P. Kerschbaum, W. E. Marshall, and R. E. Moon, "Development of Armco Direct Reduction Process," *Proc. Ironmaking Conference, AIME*, 28, 400 (1969).

Labee, C. J., "Armco's Direct Reduction Facility Operating at full Production," *Iron and Steel Engineer*, 73 (Nov., 1974).

Lownie, H. W., Jr., and T. M. Barnes, "Techniques and Economics for the Direct Reduction of Iron Ore," American Chemical Society Annual Meeting, Boston, Mass (Apr. 13, 1972).

Mackenzie, J., "A Review of Direct Reduction Processes," *Proceedings of the Symposium on Chemical Engineering in the Metallurgical Industries*, Edinburgh, Scotland (Sept., 1963).

McGannon, H. E., ed., *The Making, Shaping and Treating of Steel*, 9 ed., United States Steel Corporation (1971).

Miller, J. R., "The Inevitable Magnitudes of Metallized Iron Ore," *Iron and Steel Engineer*, 41 (Dec., 1972).

Miller, R. L., "Adiabatic Model for Hematite Reduction in Counter-Current and Packed Beds," Ph.D. thesis, Carnegie-Mellon Univ., Pittsburgh, Pa. (1972).

Perry, J. H., ed., *Chemical Engineer's Handbook*, 4 ed., McGraw-Hill, New York (1963).

Pitt, R. S., "Direct Reduction of Iron Ore, Part 1: Direct Reduction Processes and Their Energy Sources," *Iron and Steel International*, 242 (1973*a*).

———, "Direct Reduction of Iron Ore, Part 2: The Use of Direct-Reduced Material for Iron and Steelmaking," *ibid.*, 347 (1973*b*).

Ray, W. H., and J. Szekely, *Process Optimization*, Wiley, New York (1973).
Spitzer, R. H., F. S. Manning, and W. O. Philbrook, "Simulation of Topochemical Reduction of Hematite via Intermediate Oxides in an Isothermal Counter-current Reactor," *TMS-AIME*, **242**, 618 (1968).
Tsay, Q. T., "Modeling and Optimization of Direct Reduction Process Carried Out in a Shaft Furnace Arrangement," Ph.D. thesis, State University of New York at Buffalo (1975).
Weast, R. C., ed., *Handbook of Chemistry and Physics*, 54 ed., Chemical Rubber Publishing Company, Cleveland, Ohio (1973).
Yagi, J., R. Takahashi, and Y. Omori, "Study on the Reduction Process of Iron Oxide Pellets in Isothermal Fixed Bed," *Sci. Rep. RITU.*, **A23**, 31 (1971).
Yagi, J., "Process Simulation of Nonisothermal Fixed Bed for Noncatalytic Reaction," *Trans. ISIJ*, **14**, 17 (1974).

Manuscript received July 12, and accepted September 1, 1976.

Enzymatic Regeneration of ATP

ROBERT S. LANGER
BRUCE K. HAMILTON
COLIN R. GARDNER
MICHAEL C. ARCHER
and
CLARK K. COLTON

Department of Chemical Engineering
Massachusetts Institute of Technology
Cambridge, Massachusetts 02139

I. Alternative Routes

Prospects for enzymatic synthesis processes on an industrial scale depend upon development of a practical process for ATP regeneration. The relative merits of various routes to ATP regeneration involving chemical synthesis, whole cells or organelles, or cell free enzymes are evaluated. The most promising route involves one or more enzymes incorporating the reaction catalyzed by acetate kinase for ADP phosphorylation.

SCOPE

Recent advances in the immobilization and stabilization of enzymes have greatly enhanced their potential for use as highly specific catalysts in large scale industrial processes. However, the application of enzymes to processes of commercial interest has thus far been limited to degradative reactions and simple transformations. Among the more exciting but as yet unexplored applications are those which involve synthesis of complicated molecules from simpler starting materials. The specificity and selectivity offered by enzymatic catalysis cannot generally be equaled by conventional chemical synthesis or fermentation for many biologically, medicinally, and nutritionally important classes of compounds.

Adenosine 5′-triphosphate (ATP) plays a prominant role in many enzymatic pathways such as synthesis of polysaccharides, lipids, polypeptides, and nucleic acids. In these reactions, otherwise thermodynamically unfavorable syntheses are driven to completion by coupling with the degradation of ATP to adenosine 5′-diphosphate (ADP), adenosine 5′-monophosphate (AMP), or adenosine. The need to regenerate expensive ATP represents a technical and economic barrier to the development of enzyme synthetic processes.

Although several approaches for ATP regeneration have been suggested, no attempt has previously been made to systematically evaluate the many alternatives which may be conceived. In this paper we examine a wide variety of routes to ATP regeneration and discuss their relative merits for use in a large scale commercial process.

CONCLUSIONS AND SIGNIFICANCE

Potential routes for ATP regeneration involve chemical synthesis, whole cells and organelles, or cell free enzymes. Specific examples in these categories are examined in view of the major determinants of cost for a practical process.

All useful chemical syntheses involve nonaqueous media, expensive reagents in stoichiometric excess, and production of useless side products. Intact or disrupted cell preparations provide greater selectivity but are inefficient in the use of a fuel source (glucose). Conversely, subcellular organelles which are responsible for biological ATP regeneration, such as mitochondria, chloroplasts, and chromatophores, are the most efficient in their use of reactants, but their useful lifetime is too short for a practical process.

Correspondence concerning this paper should be addressed to C. K. Colton. R. S. Langer is with the Children's Hospital Medical Center, Boston, Massachusetts. B. K. Hamilton is with the Frederick Cancer Research Center, Frederick, Maryland. C. R. Gardner is with the Centre de Recherche Merrell International, Strasbourg, France. M. C. Archer is with the Dept. of Nutrition and Food Science, Massachusetts Institute of Technology, Cambridge, Massachusetts.